

## Breakdown of Fourier's Law in Nanotube Thermal Conductors

C. W. Chang,<sup>1,2,\*</sup> D. Okawa,<sup>1</sup> H. Garcia,<sup>1</sup> A. Majumdar,<sup>2,3,4</sup> and A. Zettl<sup>1,2,4,+</sup>

<sup>1</sup>*Department of Physics, University of California at Berkeley, California 94720, USA*

<sup>2</sup>*Center of Integrated Nanomechanical Systems, University of California at Berkeley, California 94720, USA*

<sup>3</sup>*Departments of Mechanical Engineering and Materials Science and Engineering, University of California at Berkeley, California 94720, USA*

<sup>4</sup>*Materials Sciences Division, Lawrence Berkeley National Laboratory, Berkeley, California 94720, USA*

(Received 11 March 2008; revised manuscript received 9 July 2008; published 15 August 2008)

We present experimental evidence that the room temperature thermal conductivity ( $\kappa$ ) of individual multiwalled carbon and boron-nitride nanotubes does not obey Fourier's empirical law of thermal conduction. Because of isotopic disorder,  $\kappa$ 's of carbon nanotubes and boron-nitride nanotubes show different length dependence behavior. Moreover, for these systems we find that Fourier's law is violated even when the phonon mean free path is much shorter than the sample length.

DOI: [10.1103/PhysRevLett.101.075903](https://doi.org/10.1103/PhysRevLett.101.075903)

PACS numbers: 65.80.+n, 63.22.Gh, 73.63.Fg, 74.25.Kc

In analogy to Ohm's law for electrical conductors, Fourier's law is an empirical rule of heat transfer in solids which states that the thermal conductance of a material scales inversely with its length or, equivalently, that the thermal conductivity is independent of sample length. Although Fourier's law is well established for virtually all thermal conductors that have been experimentally examined, efforts towards providing a rigorous theoretical basis for it have failed [1]. Theoretical studies over the past decade have demonstrated that Fourier's law is violated for a variety of one-dimensional systems [2]. Unfortunately, despite these intriguing models, the validity criteria for Fourier's law remain elusive, and a breakdown of Fourier's law seems to be commonplace [3]. Various criteria such as a temperature gradient [4], disorder [5], or anharmonicity [2] are poor predictors for Fourier's law to hold, even in one dimension.

An experimental investigation of the validity of Fourier's law in one dimension is exceptionally challenging. The difficulty lies primarily with the technique associated with measuring thermal conductivity ( $\kappa$ ) of one-dimensional, nanoscale materials, with the added complexity of systematically varying the size of the investigated object [6,7]. The dearth of relevant experimental data has restricted the one-dimensional Fourier's law problem effective to theoretical investigations, beginning with the pioneering work of Peierls [8].

Carbon nanotubes (CNTs) and boron-nitride nanotubes (BNNTs) are one-dimensional materials.  $\kappa$  of CNTs has been demonstrated to be dominated by phonons [9,10], while for BNNTs it is exclusively due to phonons [11]. Thus, nanotubes are model systems ideally suited for experimental investigations of the validity of Fourier's law in a low dimension. We here report on measurements of thermal conductivity of CNTs and BNNTs as a function of sample length. In both cases we find an unmistakable deviation from Fourier's law.

Multiwalled CNTs having diameters ranging from 10 to 33 nm were prepared using conventional arc methods [12]. Multiwall BNNTs were synthesized using an adaptation of a previously reported method, yielding samples with a typical outer diameter of 30–40 nm and a length of  $\sim 10 \mu\text{m}$  [13]. Individual multiwall tubes were placed on a custom-designed microscale thermal conductivity test fixture using a piezo-driven manipulator operated inside a scanning electron microscopy (SEM). The fixture incorporated independently suspended  $\text{SiN}_x$  pads, with integrated Pt film resistors serving as either heaters or sensors (i.e., thermometers) [14]. The thermal conductance of a nanotube was determined after supplying power to the heater and measuring the resulting temperature changes of the heater and sensor pads. The test fixture was also made compatible with operation within a high-resolution transmission electron microscope so that the geometrical factors of the nanotube under study could be precisely determined.

Several options are available to the experimenter in determining the transport coefficients for a one-dimensional system with finite contact resistance. In the traditional method, the sample is mounted at one end, and a second movable probe is used as a local probe. Although this method is well suited for diffusive transport, it cannot determine the transport coefficients if the sample is a ballistic conductor with unknown contact resistances. Here we utilize a different kind of sequential multiprobe method that can establish a sample's deviation from Fourier's law behavior even for nanoscale samples with possible ballistic conduction. The method also accounts for finite contact resistances.

The upper part of Fig. 1 outlines the experimental procedure, in this case for a BNNT. The inset in Fig. 1 shows the nanotube attached to the test fixture via two roughly square-shaped contacts; these are formed from (trimethyl) methylcyclopentadienyl platinum  $[(\text{CH}_3)_3(\text{CH}_3\text{C}_5\text{H}_4)\text{Pt}]$  inside the SEM. The right contact attaches the nanotube

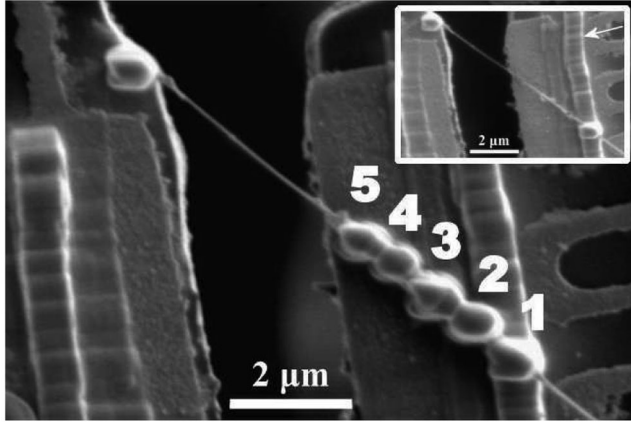
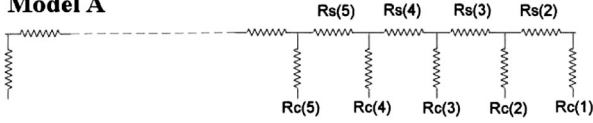
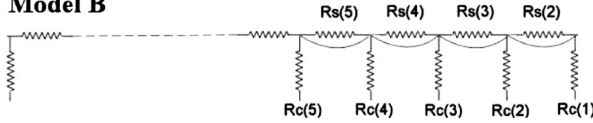
**Model A****Model B**

FIG. 1. Upper: A SEM image of a thermal conductivity test fixture with a BNNT (BNNT sample 1) after five sequences of  $(\text{CH}_3)_3(\text{CH}_3\text{C}_5\text{H}_4)\text{Pt}$  deposition. The numbers denote the  $n$ th deposition. The inset shows the SEM image after the first  $(\text{CH}_3)_3(\text{CH}_3\text{C}_5\text{H}_4)\text{Pt}$  deposition. The arrow denotes the preformed rib for suspending the BNNT. Lower: Two circuit models for analyzing the data of BNNT sample 1.  $R_s(n)$  and  $R_c(n)$  denote the sample resistance and the contact resistance at each deposition, respectively.

to the top of a preformed vertical “rib” (identified with an arrow) on the right thermal pad; this elevation ensures that the nanotube is fully suspended along its entire length between the contacts. The thermal conductance of the sample spanning the thermal pads is then measured. Following measurement, an additional thermal contact post is deposited, again using  $(\text{CH}_3)_3(\text{CH}_3\text{C}_5\text{H}_4)\text{Pt}$ , inward of the original right-hand contact. This additional contact post is denoted “2” in the upper part of Fig. 1. The thermal conductance is again measured. This process is repeated with a series of additional  $(\text{CH}_3)_3(\text{CH}_3\text{C}_5\text{H}_4)\text{Pt}$  depositions, as denoted by the numbers in the upper part of Fig. 1. Each deposition makes a new, additional thermal contact to the nanotube and reduces the suspended segment of the nanotube. Although high-resolution transmission electron microscope images show that there are some residues of  $(\text{CH}_3)_3(\text{CH}_3\text{C}_5\text{H}_4)\text{Pt}$  deposited along the nanotube, control experiments show that the residues contribute less than 2% of the total thermal conductance.

The analysis of nanotube thermal conductance versus sample length would be trivial were it not for the finite contact resistance between the nanotube and the test fixture

thermal pads. The lower part of Fig. 1 shows two thermal circuit models that we employ to analyze the above contacting sequence. In model A the thermal resistance of the sample between each contact post is equivalent to a series of resistors  $R_s(n)$  ( $n =$  sequence number) connected to each other, with contact resistance  $R_c(n)$  representing each  $(\text{CH}_3)_3(\text{CH}_3\text{C}_5\text{H}_4)\text{Pt}$  deposition connected in parallel to the  $R_s(n)$ 's. During the analysis, each  $R_s(n)$  and  $R_c(n)$  is adjusted for the corresponding geometrical factor, i.e.,  $R_s = R_s l(n)^{1-\beta}$  and  $R_c(n) = R_c/l(n)$ , where  $l(n)$  is the length of the  $n$ th contact. In each sequence, the total resistance  $R_{\text{total}}(n)$  satisfies the following iteration relation:

$$R_{\text{link}}(1) = R_c(1);$$

$$R_{\text{link}}(n) = \frac{R_c(n)[R_s(n) + R_{\text{link}}(n-1)]}{R_s(n) + R_c(n) + R_{\text{link}}(n-1)};$$

$$R_{\text{total}}(n) = R_s \left( L_s - \sum_{k=1}^n l(k) \right)^{1-\beta} + R_{\text{link}}(n) + R_c(\text{left}),$$
(1)

where  $L_s$  is the sample length before depositing the first contact post and  $R_c(\text{left})$  denotes the contact resistance of the left contact post shown in Fig. 1 [15]. We have also considered model B, where the contacts are shorted to each other. Figure 2 shows the normalized thermal resistance

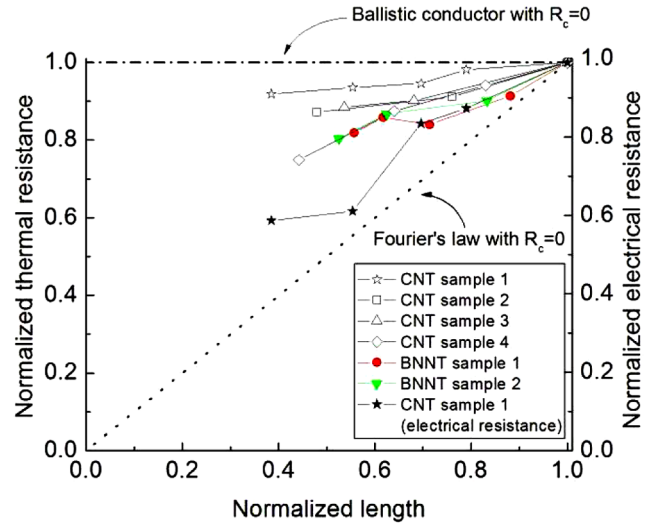


FIG. 2 (color online). Normalized resistance vs normalized sample length for different CNT and BNNT samples. The result of a ballistic conductor with  $R_c(n) = 0$  is shown as the dashed-dotted line. The result of Fourier's law with  $R_c(n) = 0$  is shown as the dotted line. The (thermal resistance, length) for each sample are, respectively, normalized to: CNT sample 1:  $(3.93 \times 10^7 \text{ K/W}, 5.38 \mu\text{m})$ ; CNT sample 2:  $(3.34 \times 10^7 \text{ K/W}, 3.84 \mu\text{m})$ ; CNT sample 3:  $(6.24 \times 10^7 \text{ K/W}, 3.73 \mu\text{m})$ ; CNT sample 4:  $(5.87 \times 10^7 \text{ K/W}, 5.00 \mu\text{m})$ ; BNNT sample 1:  $(2.12 \times 10^7 \text{ K/W}, 7.01 \mu\text{m})$ ; BNNT sample 2:  $(7.71 \times 10^7 \text{ K/W}, 5.33 \mu\text{m})$ . The electrical resistance for CNT sample 1 is normalized to 98.2 K $\Omega$ .

with respect to normalized sample length for several isotopically unmodified CNTs and BNNTs. Notably, when  $R_c(n) = 0$ , a ballistic conductor yields the dashed-dotted line in Fig. 2 and lies below the dashed-dotted line when  $R_c(n) > 0$ . In contrast, when  $R_c(n) = 0$ , Fourier's law yields the dotted line in Fig. 2 and generally encompasses the region below the dotted line when  $R_c(n) > 0$ . Because the experimental data for CNTs and BNNTs consistently fall above the dotted line, Fig. 2 clearly demonstrates that Fourier's law is violated in nanotubes.

A violation of Fourier's law can be quantified by parametrizing the sample thermal conductivity as  $\kappa \sim L^\beta$  ( $L$  is the length of the nanotube;  $\beta = 0$  corresponds to Fourier's law). To evaluate  $\beta$ , we employ a computer program that searches the parameter space spanned by  $R_s$  and  $R_c$  to establish the minimum deviation from the experimentally determined  $\kappa$  value. The deviation ( $\sigma$ ) is defined as

$$\sigma = \sum_{n=1}^m [R_{\text{mea}}(n) - R_{\text{fit}}(n)]^2, \quad (2)$$

where  $m$  is the total sequence number.  $R_{\text{mea}}(n)$  and  $R_{\text{fit}}(n)$  are the normalized measured thermal resistance and the fitting result at each sequence, respectively.

Figures 3(a) and 3(b) show the fitting results using model A for CNT sample 4 and BNNT sample 2. It is clear

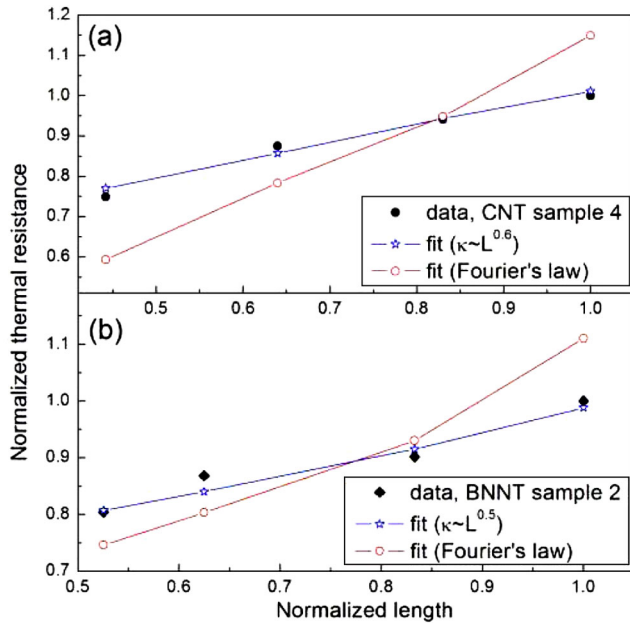


FIG. 3 (color online). (a) Normalized thermal resistance vs normalized sample length for CNT sample 4 (solid black circles), best fit assuming  $\beta = 0.6$  (open blue stars), and best fit assuming Fourier's law (open red circles). (b) Normalized thermal resistance vs normalized sample length for BNNT sample 2 (solid black diamonds), best fit assuming  $\beta = 0.4$  (open blue stars), and best fit assuming Fourier's law (open red circles).

that Fourier's law ( $\beta = 0$ ) provides a poor fit to the experimental data. The best fit occurs at  $\beta = 0.6$  for CNT sample 4 and  $\beta = 0.5$  for BNNT sample 2, respectively. From the best fit, we find that the thermal conductances are  $2.3 \times 10^{-8}$  and  $1.7 \times 10^{-8}$  W/K for CNT sample 4 and BNNT sample 2, respectively. The contact resistance of the first  $(\text{CH}_3)_3(\text{CH}_3\text{C}_5\text{H}_4)\text{Pt}$  deposition contributes less than 28% and 25% to the original intrinsic sample resistance of CNT sample 4 and BNNT sample 2, respectively.

To check the fidelity of the circuit models as applied to the thermal nanotube system, we have employed a similar analysis to the concurrently measured electrical resistance for CNT sample 1 (this is not possible for BNNTs, as they are electrical insulators). The room temperature electrical resistance of a multiwalled CNT of the dimensions used here has been demonstrated to be diffusive [16,17]. The inset in Fig. 4(a) shows the corresponding variation of  $\sigma$  with respect to  $\beta$  based on model A for electrical resistance of CNT sample 1. The minimum occurs at  $\beta = 0.2$ . In contrast, the simultaneous thermal conductance measurement of CNT sample 1 shows the minimum  $\sigma$  occurring at  $\beta = 0.8$  [Fig. 4(a), main body]. Although the fitting result for electrical resistance is close to Ohm's law, it also suggests that model A might overestimate  $\beta$ . We have also checked the results from model B; in general, model B gives a higher  $\beta$  (i.e., a larger deviation from Fourier's law) than does model A.

We have repeated the above experiments and analyses for different BNNT and CNT samples. Generally, we find that for CNTs the minimum  $\sigma$  occurs at  $\beta = (0.6-0.8)$ ,

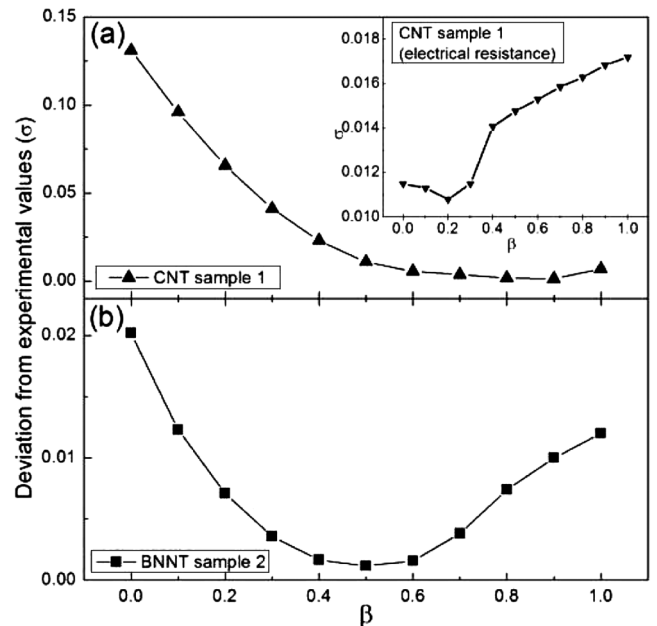


FIG. 4. Calculated deviation ( $\sigma$ ) with respect to  $\beta$  for thermal resistance of (a) CNT sample 1 (up triangles) and (b) BNNT sample 2 (squares). The inset shows  $\sigma$  vs  $\beta$  for electrical resistance of CNT sample 1 (down triangles).

whereas for BNNTs the minimum  $\sigma$  occurs at  $\beta = (0.4-0.6)$ . This difference may reflect the difference in isotopic disorder between BNNTs and CNTs. For BNNTs, the natural abundance boron has large isotopic disorder (19.9%  $^{10}\text{B}$  and 80.1%  $^{11}\text{B}$ ) and affects the value of  $\kappa$  dramatically [11]. Our results are consistent with theoretical predictions that isotopic disorder does not change the divergence of  $\kappa$  in favor of Fourier's law but instead reduces the value of  $\beta$  [18].

Traditionally, the phonon mean free path ( $l_{\text{ph}}$ ) is a characteristic length scale beyond which phonons scatter and lose their phase coherence. In two- or three-dimensional systems, this definition successfully gives Fourier's law when  $L \gg l_{\text{ph}}$ . However, it has been pointed out that many one-dimensional models do not obey Fourier's law even when the  $L$  is much larger than  $l_{\text{ph}}$  [19–22]. Experimentally, the particular one-dimensional effect can be seen if we employ the relation  $\kappa = Cv l_{\text{ph}}$  to estimate  $l_{\text{ph}}$ , where  $C$  and  $v$  are, respectively, the specific heat and the averaged sound velocity  $\sim 15$  km/s, and we obtain  $l_{\text{ph}} = 20-50$  nm, which is much smaller than the length scale ( $L = 3.7-7$   $\mu\text{m}$ ) in which the violation of Fourier's law is observed. Unlike Si thin films, such a large discrepancy cannot be explained by phonon dispersion alone [23]. Therefore, we experimentally demonstrate that  $L < l_{\text{ph}}$  is not a necessary condition for violating Fourier's law in one-dimensional systems.

The observed  $\beta = (0.6-0.8)$  on multiwalled CNTs differs from theoretical predictions on single-walled CNTs of  $\beta = 0.3-0.4$  [20,24]. But it should be noted that, since the theory of multiple contacts connecting to a non-Fourier conductor has not been established, the analysis for the circuit models in Fig. 1 is not trivial. Strictly speaking, for a non-Fourier conductor, Eq. (1) is only approximately correct for model A when the differences of the contact resistances are small (such as our experiments). Further complexities of modeling a three-dimensional heat flow interfacing with a non-Fourier conductor may introduce more uncertainties in the above analysis. However, we emphasize that the simultaneous electrical/thermal measurement on CNT sample 1 strongly supports  $\beta$  to be nonzero.

In summary, we provide experimental evidence showing that Fourier's law is violated in multiwalled CNTs and BNNTs regardless of whether  $L \gg l_{\text{ph}}$ . We also show that a 20% isotopic disorder changes the divergence of  $\beta$ . The breakdown of Fourier's law in nanotubes indicates that thermal transport in one dimension is extraordinary and can lead to many potential applications [25–27].

This work was supported by the National Science Foundation within the Center of Integrated Nanomechanical

Systems, under Grant No. EEC-0425914. Support was also provided by the Director, Office of Energy Research, Office of Basic Energy Sciences, Materials Sciences and Engineering Division, of the U.S. Department of Energy under Contract No. DE-AC02-05CH11231. A.Z. gratefully acknowledges support from the Miller Institute for Basic Research in Science.

\*chihwei@berkeley.edu

†azettl@berkeley.edu

- [1] S. Lepri, R. Livi, and A. Politi, Phys. Rep. **377**, 1 (2003).
- [2] S. Lepri, R. Livi, and A. Politi, Phys. Rev. Lett. **78**, 1896 (1997).
- [3] F. Bonetto, J.L. Lebowitz, and L. Rey-Bellet, in *Mathematical Physics* (World Scientific, London, 2000), p. 128.
- [4] B. B. Hu, B. W. Li, and H. Zhao, Phys. Rev. E **61**, 3828 (2000).
- [5] B. W. Li, H. Zhao, and B. B. Hu, Phys. Rev. Lett. **86**, 63 (2001).
- [6] H. Y. Chiu *et al.*, Phys. Rev. Lett. **95**, 226101 (2005).
- [7] Z. L. Wang *et al.*, Appl. Phys. Lett. **91**, 123119 (2007).
- [8] R. Peierls, Ann. Phys. (Berlin) **395**, 1055 (1929).
- [9] J. Hone, M. Whitney, C. Piskoti, and A. Zettl, Phys. Rev. B **59**, R2514 (1999).
- [10] P. Kim, L. Shi, A. Majumdar, and P.L. McEuen, Phys. Rev. Lett. **87**, 215502 (2001).
- [11] C. W. Chang *et al.*, Phys. Rev. Lett. **97**, 085901 (2006).
- [12] D. T. Colbert *et al.*, Science **266**, 1218 (1994).
- [13] C. Tang, Y. Bando, T. Sato, and K. Kurashima, Chem. Commun. (Cambridge) **12**, 1290 (2002).
- [14] L. Shi *et al.*, J. Heat Transfer **125**, 881 (2003).
- [15] Because the circuit diagram is different for different samples, Eq. (1) may vary from sample to sample.
- [16] A. Bachtold *et al.*, Phys. Rev. Lett. **84**, 6082 (2000).
- [17] R. Hobara *et al.*, Jpn. J. Appl. Phys. **43**, L1081 (2004).
- [18] R. J. Rubin and W. L. Greer, J. Math. Phys. (N.Y.) **12**, 1686 (1971).
- [19] A. V. Savin and O. V. Gendelman, Phys. Rev. E **67**, 041205 (2003).
- [20] G. Zhang and B. W. Li, J. Chem. Phys. **123**, 114714 (2005).
- [21] T. Mai and O. Narayan, Phys. Rev. E **73**, 061202 (2006).
- [22] L. Yang, P. Grassberger, and B. Hu, Phys. Rev. E **74**, 062101 (2006).
- [23] Y. S. Ju and K. E. Goodson, Appl. Phys. Lett. **74**, 3005 (1999).
- [24] S. Maruyama, Physica (Amsterdam) **323B**, 193 (2002).
- [25] C. W. Chang, D. Okawa, A. Majumdar, and A. Zettl, Science **314**, 1121 (2006).
- [26] C. W. Chang, D. Okawa, H. Garcia, A. Majumdar, and A. Zettl, Phys. Rev. Lett. **99**, 045901 (2007).
- [27] C. W. Chang *et al.*, Appl. Phys. Lett. **90**, 193114 (2007).